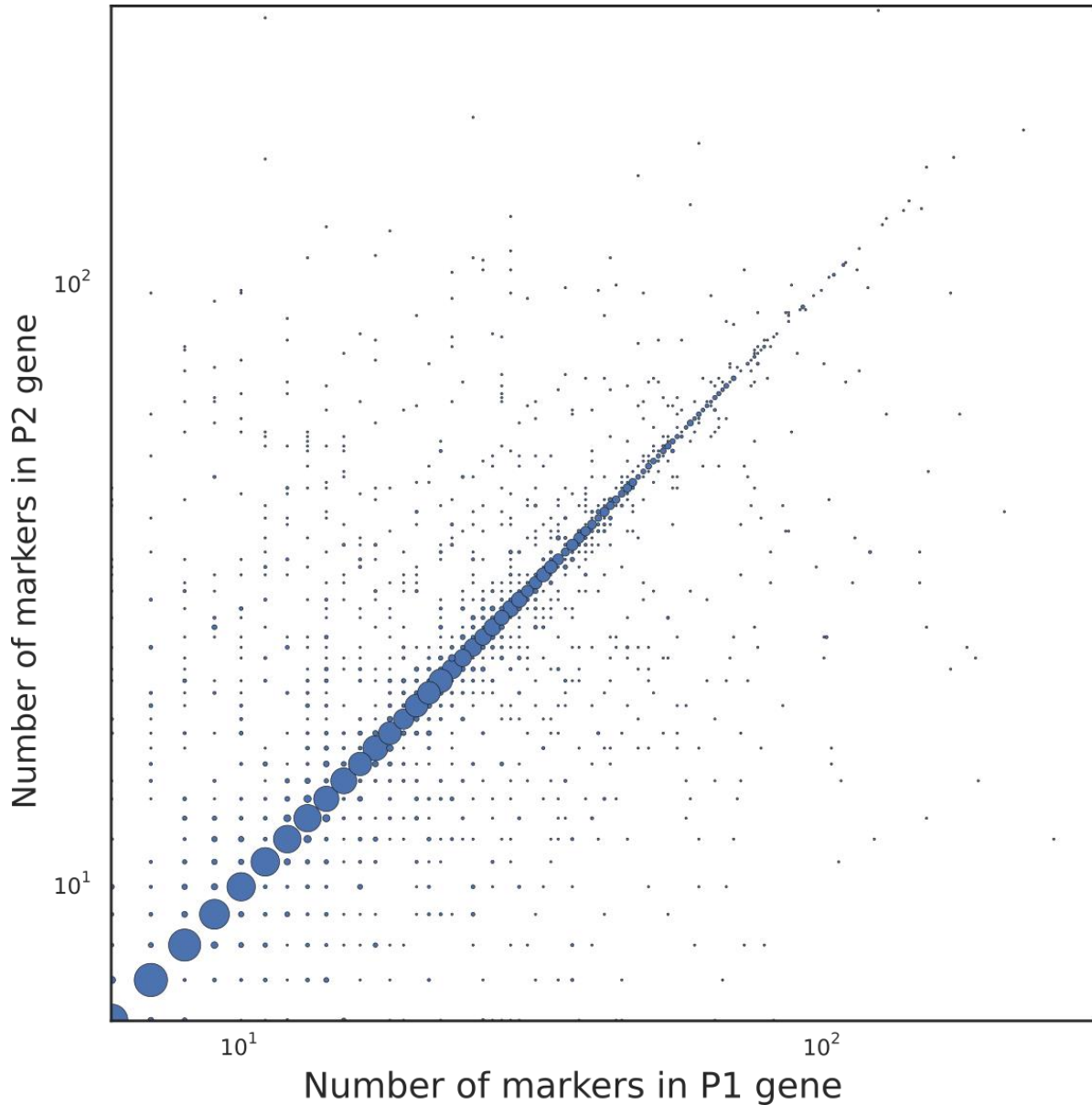


1 **Supplementary Notes for “Nucleus specific expression in the**  
2 **multinucleated mushroom *Agaricus bisporus* reveals different nuclear**  
3 **regulatory programs”**

4 Thies Gehrman, Jordi F. Pelkmans, Robin A. Ohm, Aurin M. Vos, Anton S.M. Sonnenberg, Johan J.P.  
5 Baars, Han A. B. Wösten, Marcel J. T. Reinders, Thomas Abeel

6 **Supplementary note A: The number of markers per karyollele pair**  
7 **can be asymmetric**

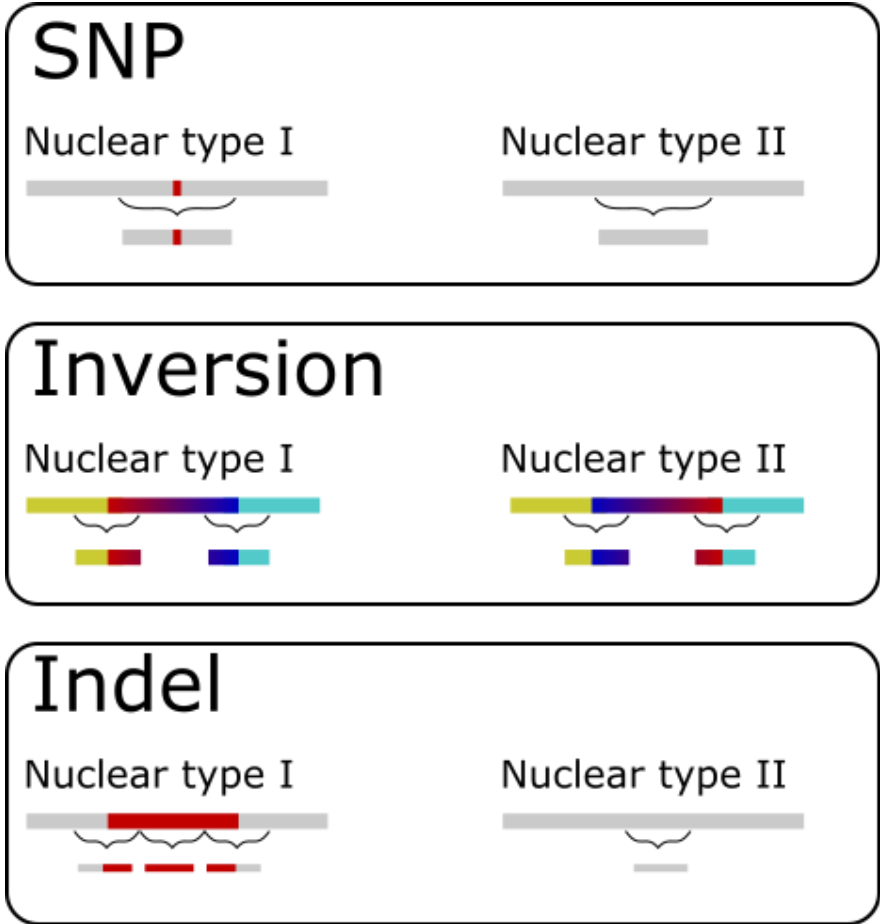
8 Most karyollele pairs have the same number of markers per karyollele. This is illustrated by large  
9 points along the diagonal of figure SF.A.1. However, some markers have different numbers of  
10 markers. Figure SF.A.2 illustrates an example of how this asymmetry occurs due to differences in the  
11 variant boundaries. Furthermore, asymmetry can also be introduced by duplication events which  
12 make markers non-unique across the rest of the genome, or even domain sequences with a  
13 mutation in one homokaryon, but not in the other.



14

15 **Figure SF.A.1: The number of karyollele pairs with a given number of markers. On the x-axis and y-axis is given the**  
16 **number of markers discovered in P1, and P2 respectively. The size of a point represents the number of karyollele pairs**  
17 **with that number of markers per homokaryon.**

18



19

20

21

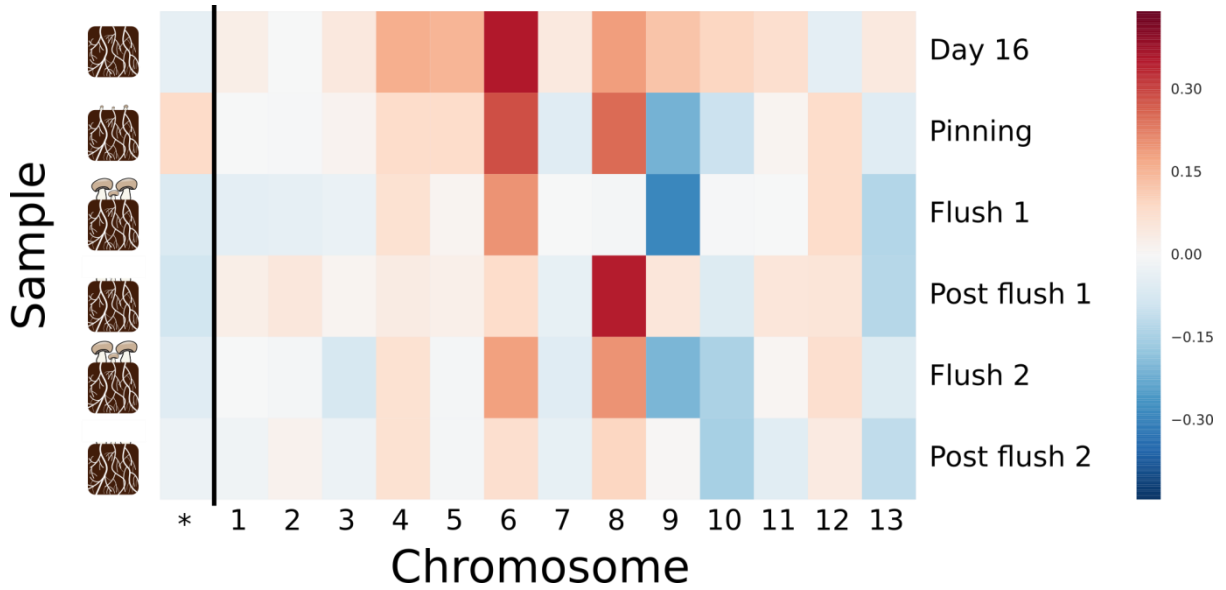
22

23

Figure SF.A.2: Different variants cause different marker counts per nuclear type. SNPs and inversions will result in an equal number of markers per nuclear type, whereas an indel can result in many more, due to the increased number of variant boundaries, and the novel sequence introduced.

24 **Supplementary Note B: Compost read ratio chromosome expression**  
25 **heatmap**

26 Figure SF.B.1 shows the Chromosome Read Ratio (CRR) measurements in compost. Notice that the  
27 scale of figure SF.B.1 is different from figures 2, 3 and 4 in the main text, but the same as SF.G.1.



28

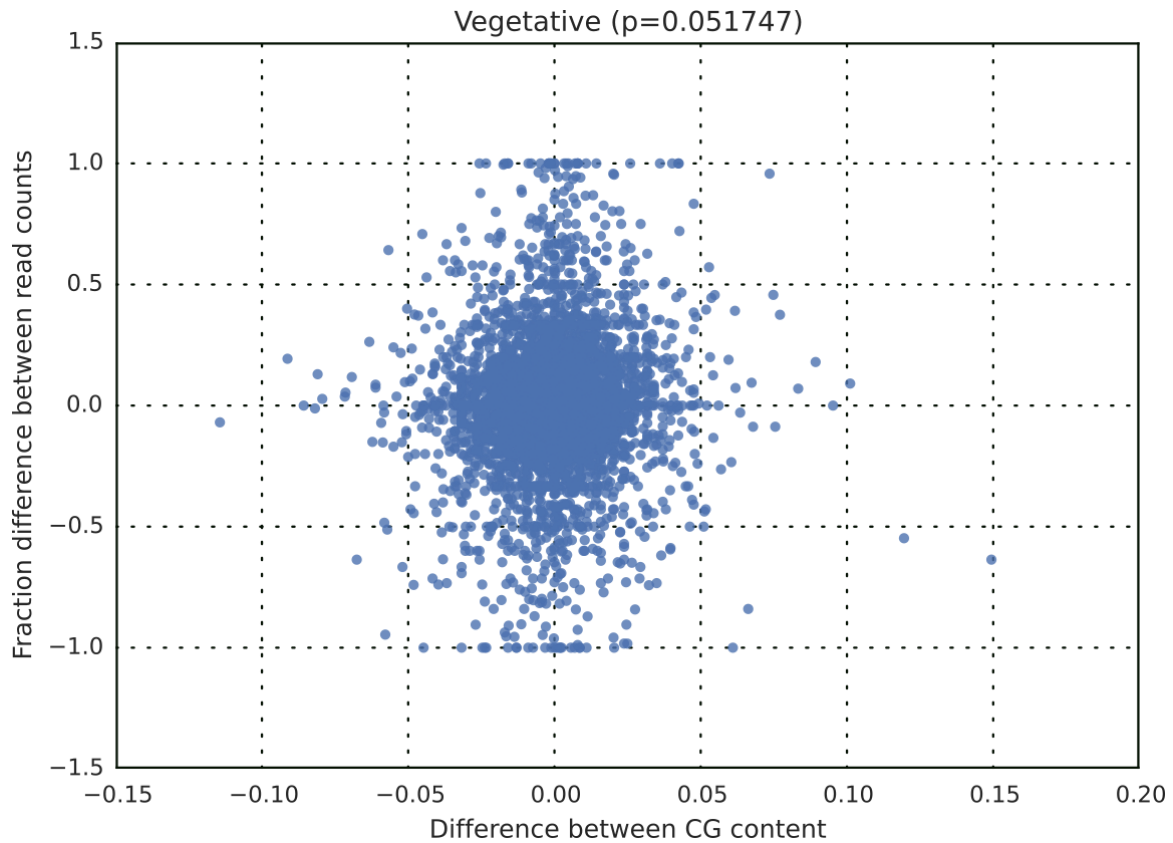
29 **Figure SF.B.1: Compost CRR measurements for each timepoint and chromosome. The first column provides the TRR**  
30 **measurements across all chromosomes. Red indicates a higher contribution of P1, and blue indicates a higher**  
31 **contribution of P2.**

32

33

34 **Supplementary Note C: Differences in CG content is not correlated to**  
35 **differences in expression**

36 Figure SF.C.1 shows the relationship between CG content and karyollele expression. For each  
37 karyollele pair, we calculate the average CG content and the average expression across all markers  
38 for each karyollele. We calculate the difference between CG contents. Additionally, the difference in  
39 read depth and normalize it to lie within [1,-1] (1 represents an entirely P1 expressed karyollele, and  
40 -1 an entirely P2 expressed karyollele, 0 represents equal expression). The difference in karyollele  
41 expression and CG content of its markers is not correlated ( $p=0.05$ )



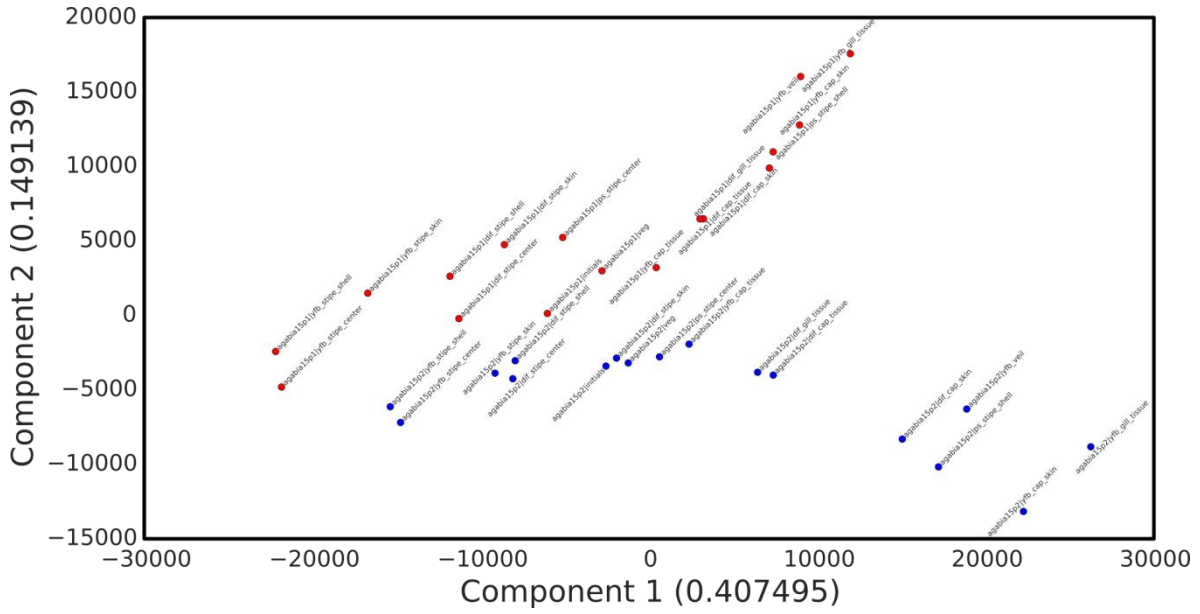
42

43 **Figure SF.C.1: Relationship between the difference in gene expression between karyollele pairs (y-axis) and average**  
44 **marker CG content per karyollele (x-axis). The average expression and average CG content of markers do not seem to be**  
45 **related. Here shown only for the vegetative stage in the mushroom dataset; Other samples show the same behaviour.**

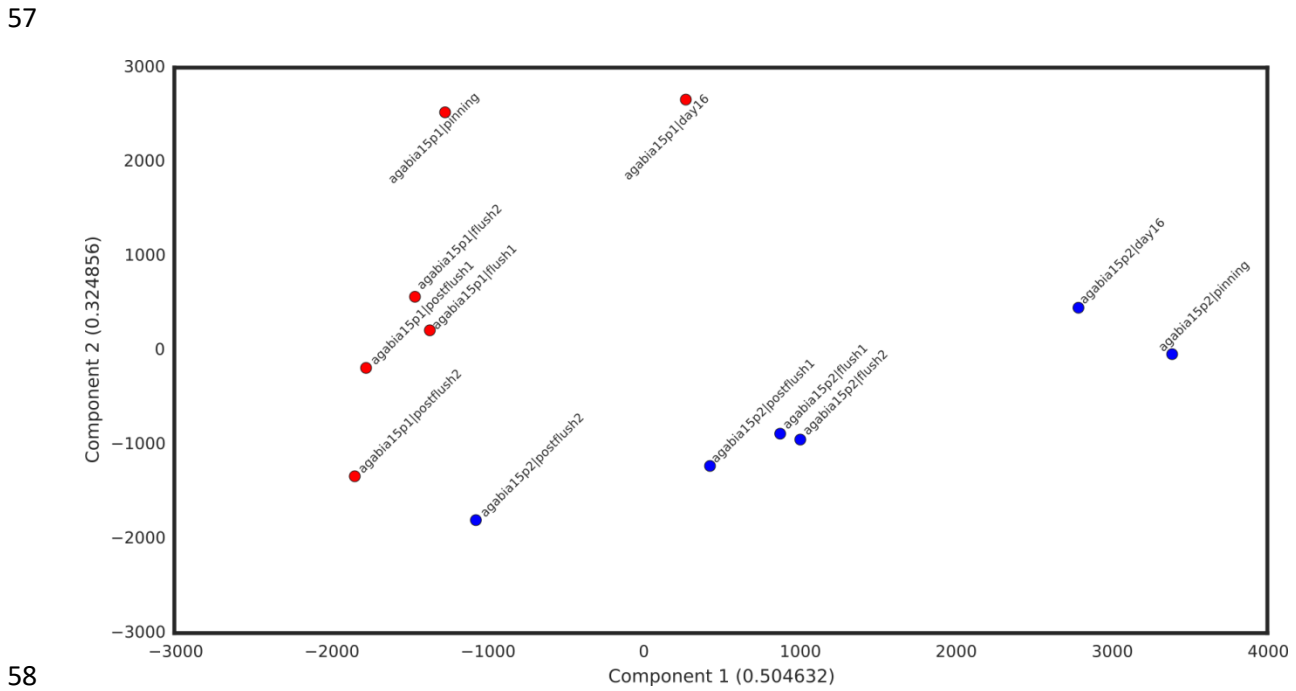
46

47 **Supplementary Note D: PCA plots of tissue and compost samples**

48 For each sample, we construct two vectors of size 5,060, describing the expression of each karyollele  
 49 in P1 and P2, respectively. With this, we perform a PCA to observe the relationships between the  
 50 different samples and nuclear types. Figure SF.D.1 shows a divergence of P1 (shown in red) and P2  
 51 (shown in blue) expression measurements in mushroom samples, indicating that P1 homokaryons  
 52 are more similar to P1 homokaryons than to any P2 homokaryon, and vice versa. Figure SF.D.2  
 53 shows the same for compost data.



54  
 55 **Figure SF.D.1: PCA dimensionality reduction of karyollele expression data. The first and second components are plotted**  
 56 **on the X and Y axes, respectively. P1 homokaryon samples are shown in red, and P2 homokaryons are shown in blue.**

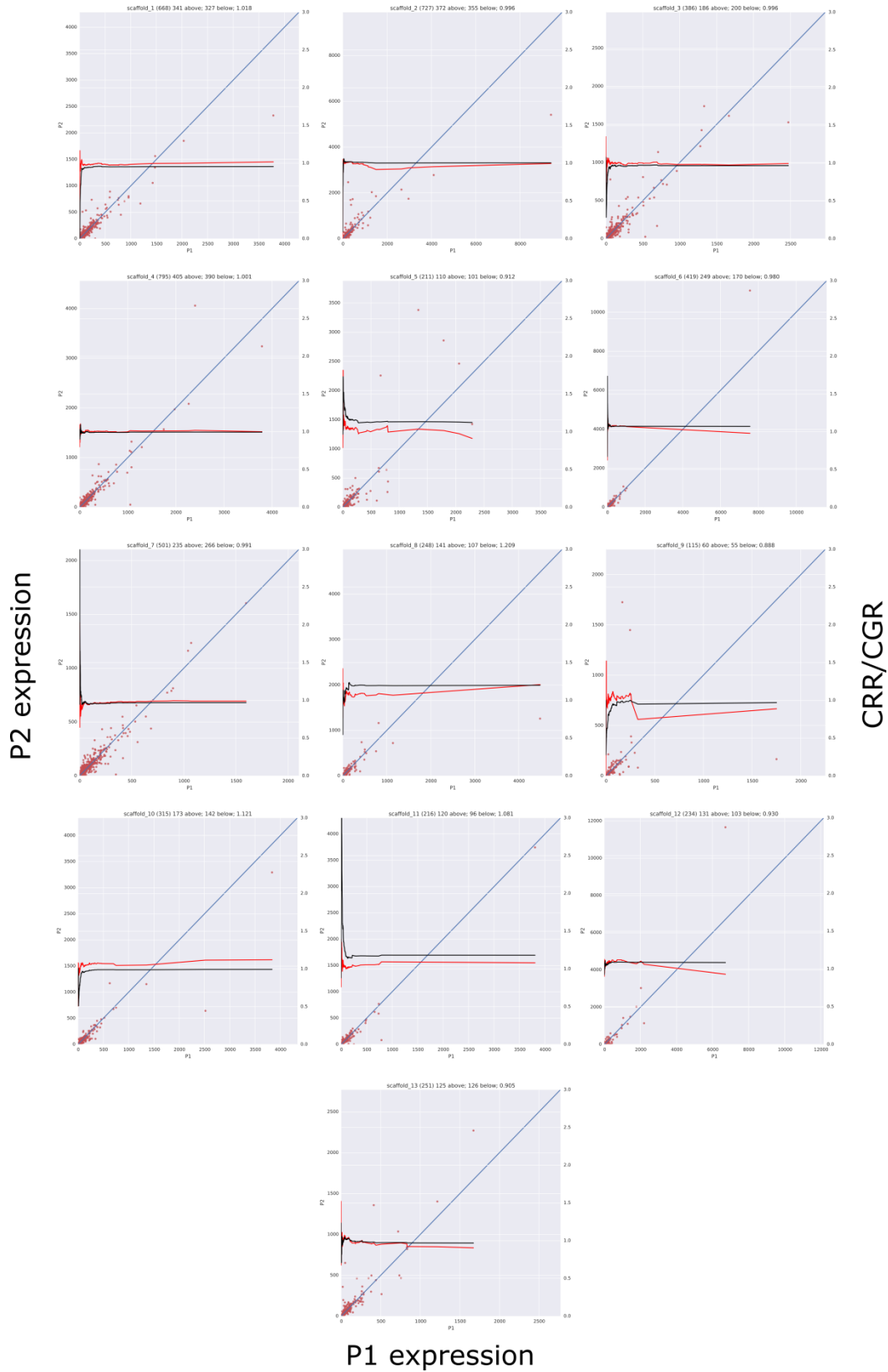


58  
 59 **Figure SF.D.2: The first and second components of a PCA are shown on the X and Y axes, respectively for compost data.**

## 60 **Supplementary Note E: Bias of extreme genes**

61 Figure SF.E.1 shows the influence of highly expressed genes on the Chromosome Read Ratio (CRR  
62 measure). We sort the genes on each chromosome based on the sum of their expression in the two  
63 nuclear types. Sorting the genes by their expression (lowest to highest), and starting with the lowest  
64 expressed gene, we calculate the CRR and CGR (Equations 4 and 6, respectively) ratios per  
65 chromosome, for increasingly larger sets of genes. We see that the CRR (red line) considerably  
66 changes once we consider highly expressed genes. The CGR (black line) is more stable towards highly

67 expressed genes.



68

69 **Figure SF.E.1: The bias of highly expressed genes. X-axis represents P1 expression, and Y-axis represents P2 expression.**  
70 **The red points represent the genes on each chromosome and their expression values in the P1 and P2 nuclear types. The**  
71 **blue line is the identity line; points on or near this line have near-identical expression. The red and black lines are the**  
72 **CRR and the CGR, with a separate y-axis on the right hand side, calculated by continuously considering the next most**



73 highly expressed gene. Read ratio is very affected by the highest expressed genes. Each chromosome is plotted  
74 individually.

## 75 **Supplementary Note F: Extreme genes**

76 In Figure 3, we showed that more mRNA originates from P2 in the case of, for example, chromosome  
77 9 than from P1. This was in part due to a few genes which were very highly expressed. These highly  
78 expressed genes skew the read count ratios (see Supplementary Material Note E). The differences  
79 can be quite extreme; In one case, a P1 karyotype accounted for <1% of all reads originating from  
80 chromosome 9, while its P2 karyotype accounted for 21% of all the chromosome 9 reads. Hence,  
81 most of the observed differences for chromosome 9 (Figure 3) is explained by such highly expressed  
82 genes.

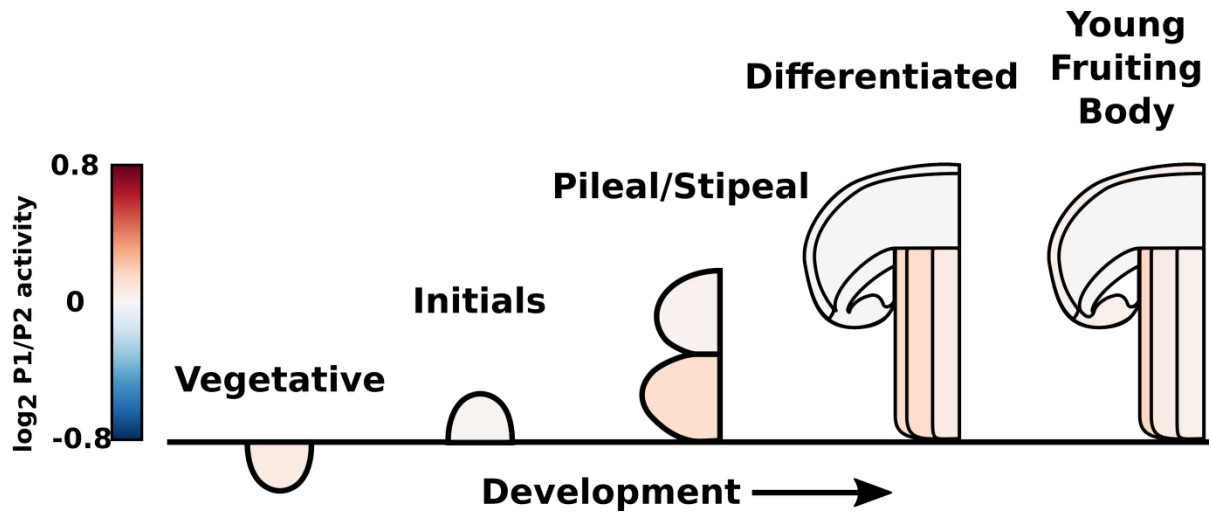
83 In total, we identified 22 genes whose contribution exceeds 10% of the total expression of the  
84 chromosome it is located on. Most of these genes are differentially expressed between the two  
85 nuclear types, with 16 showing fold changes larger than 2. These genes are primarily metabolic.

86 These genes, and their contribution to the CRR scores are provided in data sheet

87 **SupplementaryTable1.xlsx** .

88 **Supplementary note G: Nuclear type Gene Ratio (NGR) measures in**  
89 **the mushroom dataset**

90 Figure SF.G.1 shows the Nuclear type Gene Ratio measures for the mushroom dataset. It becomes  
91 clear that on average, the P1 nuclear type is dominant over the P2 nuclear type. This is statistically  
92 significant (the log-transformed chromosome gene ratios are significantly  $> 0$ , following a t-test in  
93 mushroom tissue, with  $p < 0.01$ ).

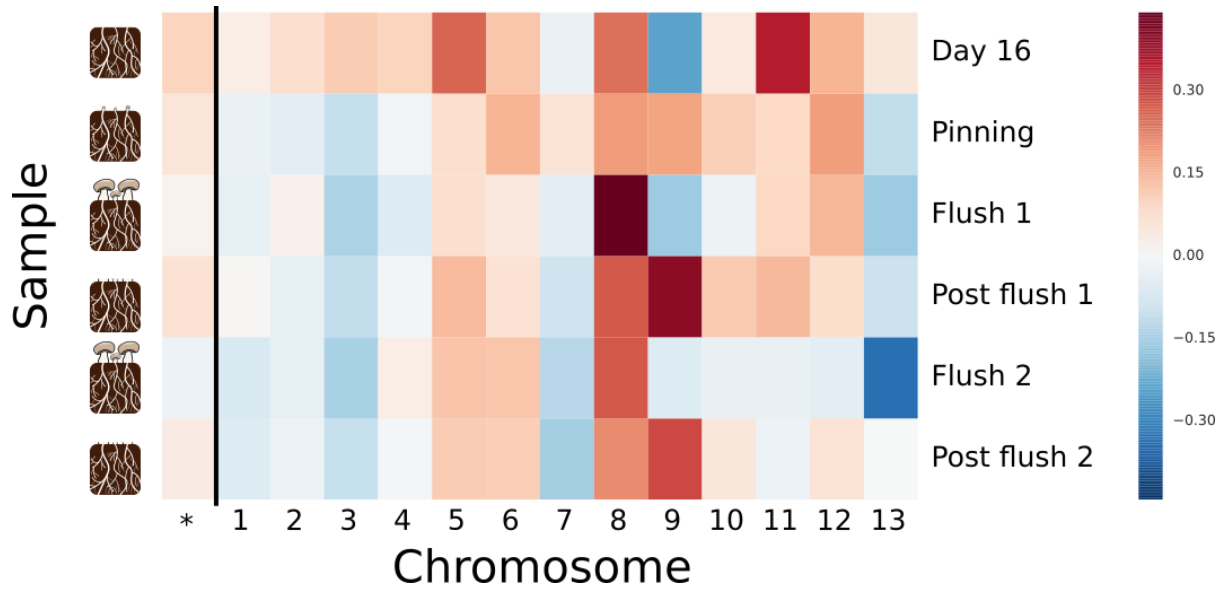


94

95 Figure SF.G.1: The Nuclear type Gene Ratio measures in the mushroom dataset.

96 **Supplementary Note H: Compost gene ratio chromosome expression**  
 97 **heatmap**

98 Figure SF.H.1 shows the Chromosome Gene Ratio measurements of each chromosome and tissue in  
 99 the compost data. Also here it is seen that the P1 homokaryon produces more mRNA per gene on  
 100 average, but it is not significantly dominant. Notice that the scale of figure SF.H.1 is different from  
 101 figures 2, 3 and 4 in the main text (but the same as SF.C.1).



102

103 **Figure SF.H.1: The Chromosome Read Gene Ratio measures for each chromosome and tissue in the compost data. Red**  
 104 **indicates a higher contribution of P1, and blue indicates a higher contribution of P2.**

105

106 **Supplementary Note I: Methylation**

107 To investigate the biological mechanism causing differential expression, we measured methylation  
 108 on the A15 genome. Assuming that the relative Cytosine/Thymine coverage at each base relates to  
 109 a differential methylation state between the two nuclear types, we conclude that 277 genes are  
 110 differentially methylated (Methods). 42 of these 277 genes were also found to be differentially  
 111 expressed between the two nuclear types at some point in development. Although this is a  
 112 significant proportion ( $p < 0.05$ ,  $\chi^2$  test), methylation only explains at most 10% of the differential  
 113 expression we observe. Noteworthy is that 40 of the 42 differentially expressed and differentially  
 114 methylated genes are differentially expressed in mushroom tissues), whereas only 9 are  
 115 differentially expressed in the vegetative mycelium. This indicates that the largest impact of  
 116 differential methylation is much later in mushroom development, suggesting that methylation has a  
 117 delayed effect on expression.

118 Table ST.I.1 shows these overlaps for the different sets of differentially expressed genes. We find  
 119 that the methylated genes overlap mostly with the genes which are differentially expressed in the  
 120 mushroom data.

121 **Table ST.I.1: Overlap of differentially expressed genes and methylated genes. The p-values of a chi-squared**  
 122 **approximation of the fisher's exact test have been bonferroni corrected (q-values). Significant corrected values have**  
 123 **been highlighted in bold.**

Set	Differentially expressed		Not Differentially Expressed		p-value	q-value
	Methylated	Not Methylated	Methylated	Not Methylated		
Vegetative mycelium + Mushroom	42	369	235	4440	1.465E-05	<b><u>8.791E-05</u></b>
Vegetative mycelium	9	73	268	4736	4.780E-02	2.868E-01
Mushroom	40	328	237	4481	3.473E-06	<b><u>2.084E-05</u></b>
Overlap	7	32	270	4777	1.937E-03	1.162E-02
Unique Vegetative mycelium	2	41	275	4768	9.150E-01	1.000E+00
Unique Mushroom	33	296	244	4513	2.493E-04	<b><u>1.496E-03</u></b>

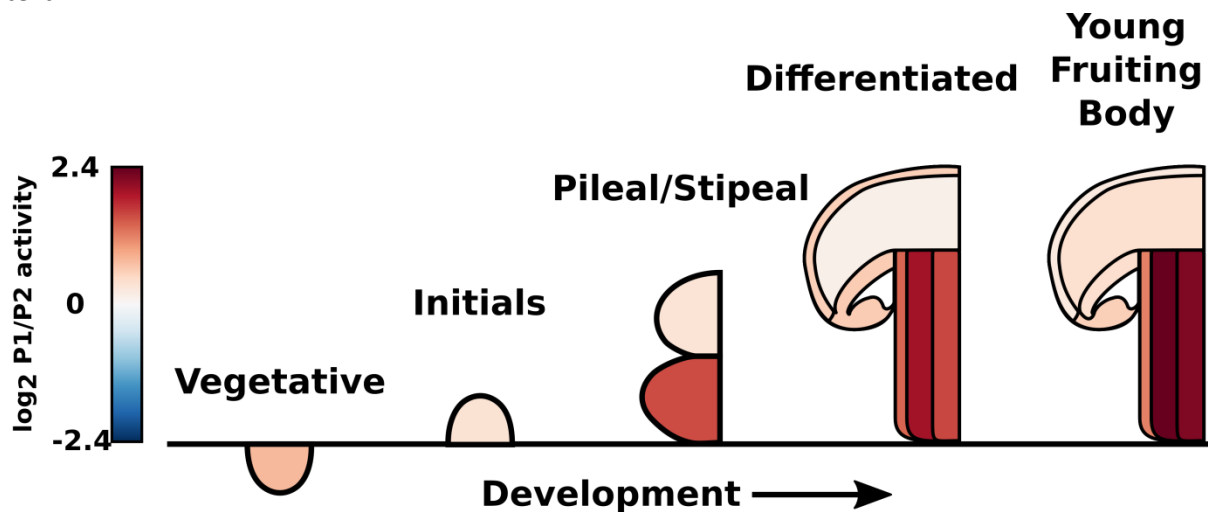
125 **Supplementary Note J: Overlapping differentially expressed genes**  
126 **that changed origin**

127 5 genes changed their differential expression between P1 and P2 between the vegetative mycelium  
128 and the mushroom datasets. These are provided in the additional data sheet:

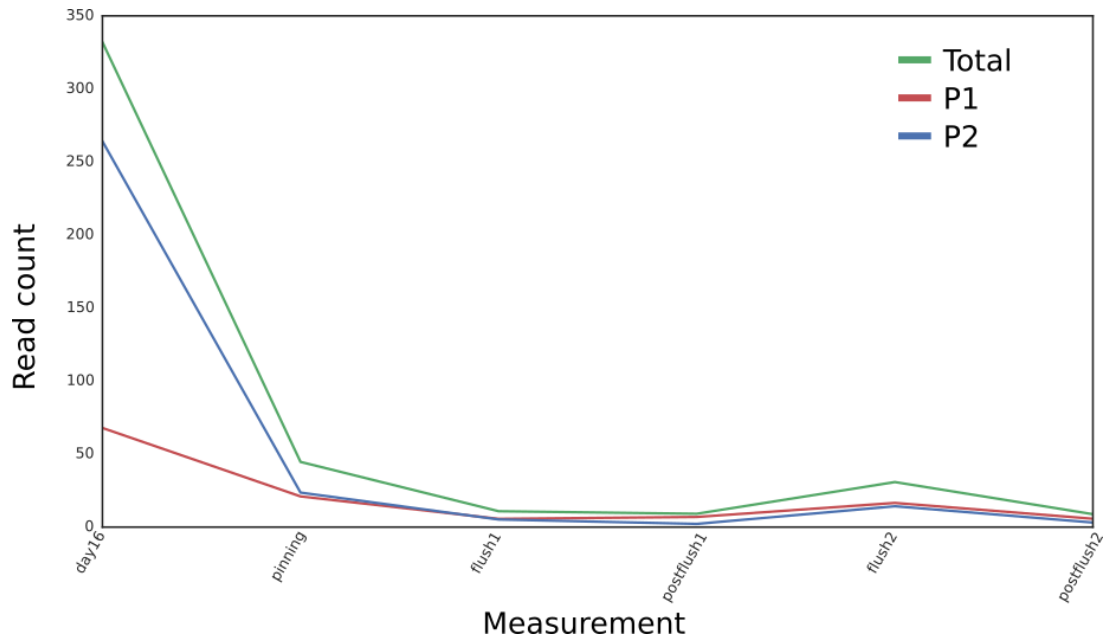
129 [SupplementaryTable2.xlsx](#) For each karyollele pair, we provide the samples for which the differential  
130 expressions were significant. The blue rows indicate the samples in which they were more highly  
131 expressed by the P2 nuclear type in the vegetative mycelium, and the red rows indicate the samples  
132 in which they were more highly expressed by the P1 nuclear type in the mushroom tissue.

133 **Supplementary Note K: Manganese Peroxidase**

134 Of 90 genes with named annotations in *A. bisporus* (see Methods), 42 are identified as differentiable  
135 karyollele pairs, and one, manganese peroxidase (*mnp1*) was differentially expressed between the  
136 two nuclear types in any stage of development. *mnp1* is known to be highly expressed in early stages  
137 of development, and drops to much lower levels (log fold change of -2.8) after mushroom  
138 formation<sup>2,28</sup>. In our datasets, the individual contributions of P1 and P2 to *mnp1* expression are  
139 largely different. In the vegetative mycelium, we find that P2 produces four-fold more *mnp1*  
140 immediately before mushroom formation than P1 (see Supplementary Material Note K). In the  
141 mushroom tissue, however, *mnp1* is expressed on average 4.2-fold higher by P1 in the stem of the  
142 fruiting body throughout development (see Supplementary Material Note K). Whether this switching  
143 behavior is functionally relevant remains unclear, as two karyolleles of *mnp1* have the same protein  
144 domain annotations in the P1 and P2 homokaryon genomes. The Gene Read Ratio (GRR) in  
145 mushroom tissues is provided in figure SF.K.1, and the total read counts in compost are provided in  
146 figure SF.K.2. Notice that the scale of figure SF.K.1 is different from figures 2, 3 and 4 in the main  
147 text.



148 Figure SF.K.1: Gene Read Ratios for Manganese Peroxidase in mushroom tissues. Red indicates a  
149 higher contribution of P1, and blue indicates a higher contribution of P2. Expression values range  
150 between [26.2,51.1] in *P1*, and between [9.3,38.2] in *P2*.  
151



152

153

154

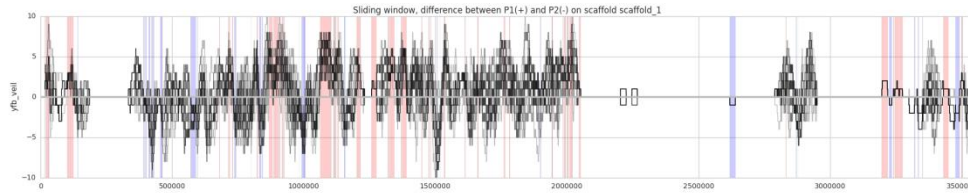
**Figure SF.K.2: Manganese peroxidase expression in the vegetative mycelium dataset. P2 expression is dominant in the vegetative growth of mycelium, but drops shortly after that, in concordance with previous literature [1].**

155

156 **Supplementary Note L: Co-localized, co-regulated clusters**

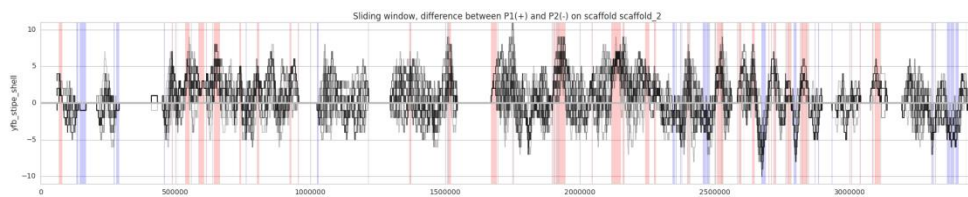
157 Figure 5 showed the co-localized and co-regulated regions on chromosome 10. In Supplementary  
158 Figures SF.L.1-13, we provide the same figures for the remaining chromosomes. Additionally, in  
159 Supplementary File SupplementaryTable3.xlsx, we provide the exact regions for each dataset.

160



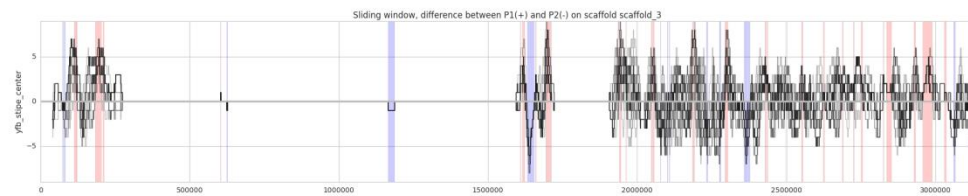
161 **Figure SF.L.1: Equation 8 plotted for all datasets on scaffold 1. Red regions indicate regions of P1 predominance, and**  
162 **blue regions indicate regions of P2 predominance.**

163



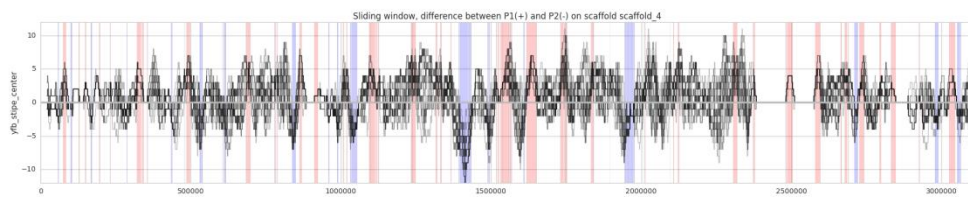
164 **Figure SF.L.2: Equation 8 plotted for all datasets on scaffold 2. Red regions indicate regions of P1 predominance, and**  
165 **blue regions indicate regions of P2 predominance.**

166



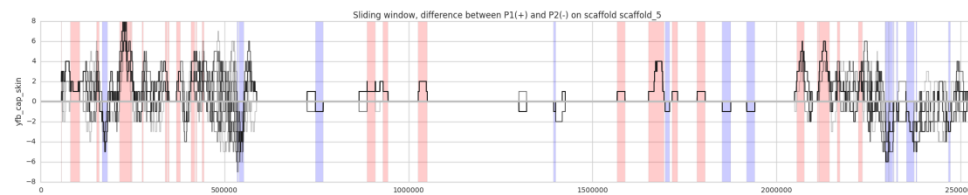
167 **Figure SF.L.3: Equation 8 plotted for all datasets on scaffold 3. Red regions indicate regions of P1 predominance, and**  
168 **blue regions indicate regions of P2 predominance.**

169



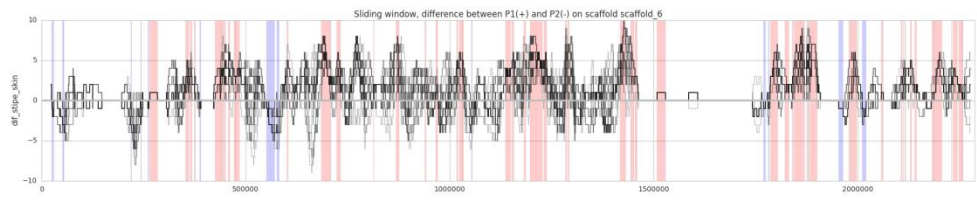
170 **Figure SF.L.4: Equation 8 plotted for all datasets on scaffold 4. Red regions indicate regions of P1 predominance, and**  
171 **blue regions indicate regions of P2 predominance.**

172

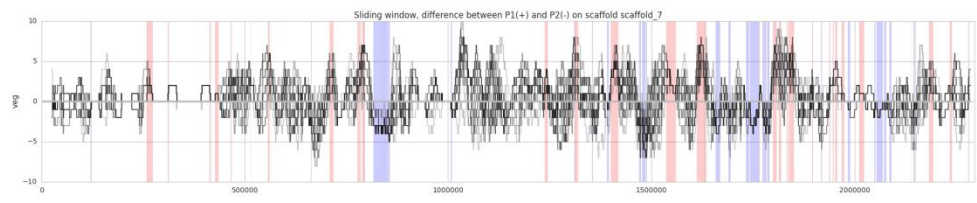




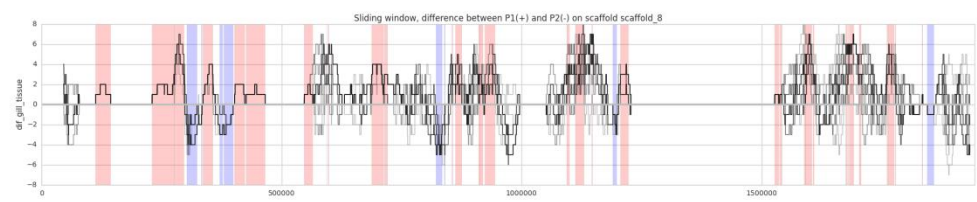
173 **Figure SF.L.5: Equation 8 plotted for all datasets on scaffold 5. Red regions indicate regions of P1 predominance, and**  
174 **blue regions indicate regions of P2 predominance.**



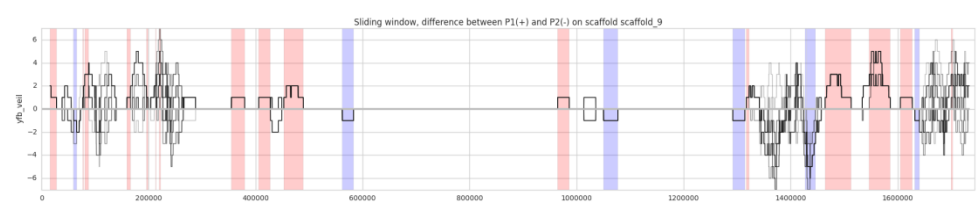
175  
176 **Figure SF.L.6: Equation 8 plotted for all datasets on scaffold 6. Red regions indicate regions of P1 predominance, and**  
177 **blue regions indicate regions of P2 predominance.**



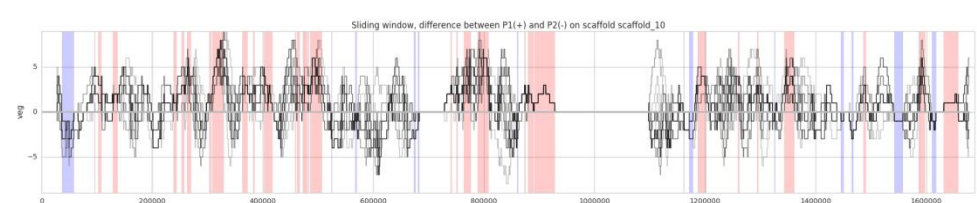
178  
179 **Figure SF.L.7: Equation 8 plotted for all datasets on scaffold 7. Red regions indicate regions of P1 predominance, and**  
180 **blue regions indicate regions of P2 predominance.**



181  
182 **Figure SF.L.8: Equation 8 plotted for all datasets on scaffold 8. Red regions indicate regions of P1 predominance, and**  
183 **blue regions indicate regions of P2 predominance.**

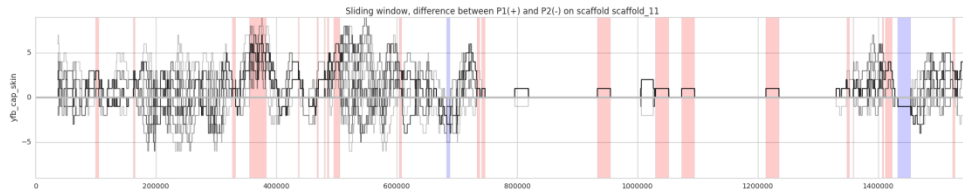


184  
185 **Figure SF.L.9: Equation 8 plotted for all datasets on scaffold 9. Red regions indicate regions of P1 predominance, and**  
186 **blue regions indicate regions of P2 predominance.**



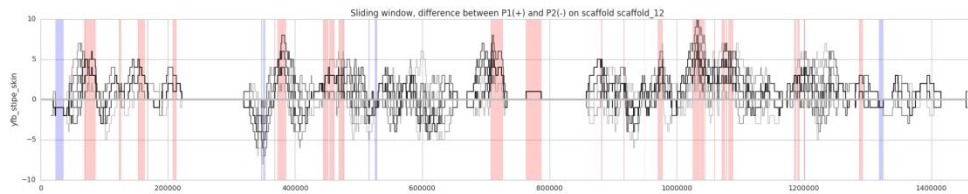
187

188 **Figure SF.L10: Equation 8 plotted for all datasets on scaffold 10. Red regions indicate regions of P1 predominance, and**  
189 **blue regions indicate regions of P2 predominance.**



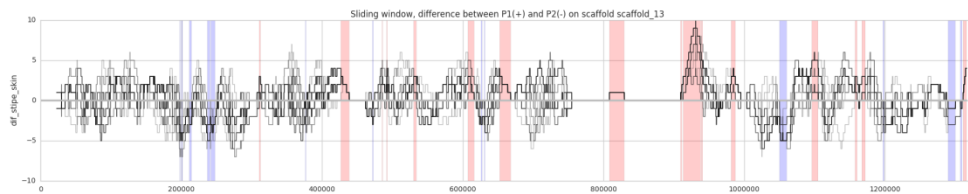
190

191 **Figure SF.L11: Equation 8 plotted for all datasets on scaffold 11. Red regions indicate regions of P1 predominance, and**  
192 **blue regions indicate regions of P2 predominance.**



193

194 **Figure SF.L12: Equation 8 plotted for all datasets on scaffold 12. Red regions indicate regions of P1 predominance, and**  
195 **blue regions indicate regions of P2 predominance.**



196

197 **Figure SF.L13: Equation 8 plotted for all datasets on scaffold 13. Red regions indicate regions of P1 predominance, and**  
198 **blue regions indicate regions of P2 predominance.**

199

200 **Supplementary Note M: Probability of observing differential**  
 201 **expression imbalance**

202 We can judge the likelihood of observing an imbalance in the number of differentially expressed  
 203 genes on the two homokaryons. For a given time point with x upregulated genes in P1, and y  
 204 upregulated genes in P2, we can determine the probability of observing max(x, y) positive trials  
 205 within x+y trials, under the null hypothesis of there being no difference in chance of a gene being  
 206 upregulated in either homokaryon (i.e. p = 0.5). The probability of observing a value max(x,y) or  
 207 greater can be calculated as 1-P(x < max(x,y)). If this probability is sufficiently small, we may reject  
 208 the underlying assumption that the probability of being upregulated is the same in both  
 209 homokaryons (i.e. p != 0). P-values are corrected by controlling for a 0.05 FDR. The difference was  
 210 only significant in some vegetative growth time points, shown underlined in ST.M.1.

211 **Table ST.M.1: The number of differentially expressed genes that are more highly expressed in P1 or P2 in each different**  
 212 **sample, together with the significance of this difference**

condition	Up in P1	Up in P2	pvalue	qvalue
Day 16	11	29	0.001111	<u>0.027768</u>
Flush 1	14	32	0.002267	<u>0.028337</u>
Total vegetative dataset	30	52	0.005319	<u>0.044323</u>
Pinning	14	29	0.006859	<u>0.044323</u>
Flush 2	20	32	0.035197	0.148658
Post Flush 2	18	30	0.029732	0.148658
Post Flush 1	14	24	0.036476	0.148658
YFB Stipe Center	72	86	0.116317	0.363492
Initials	58	50	0.193286	0.487041
Total Mushroom dataset	176	192	0.18777	0.487041
YFB Cap Tissue	91	103	0.175335	0.487041
PS Stipe Shell	63	54	0.17764	0.487041
Dif. Stipe skin	75	80	0.314999	0.504822
Dif. Cap Skin	58	60	0.391278	0.504822
YFB Veil	72	70	0.40067	0.504822
YFB Cap Skin	89	82	0.270406	0.504822
Dif. Cap Skin	63	61	0.393873	0.504822
Dif. Gill Tissue	60	59	0.427315	0.504822
Dif. Stipe Center	87	83	0.350741	0.504822
Dif. Stipe Shell	86	90	0.353185	0.504822
YFB Gill Tissue	69	65	0.332975	0.504822
YFB Stipe Skin	94	94	0.470943	0.504822
PS Stipe Center	71	77	0.282586	0.504822
Vegetative	47	42	0.262507	0.504822
YFB Stipe Shell	93	92	0.441575	0.504822

213

214

215 **Supplementary Note N: KEGG pathways with differentially expressed**  
 216 **genes**

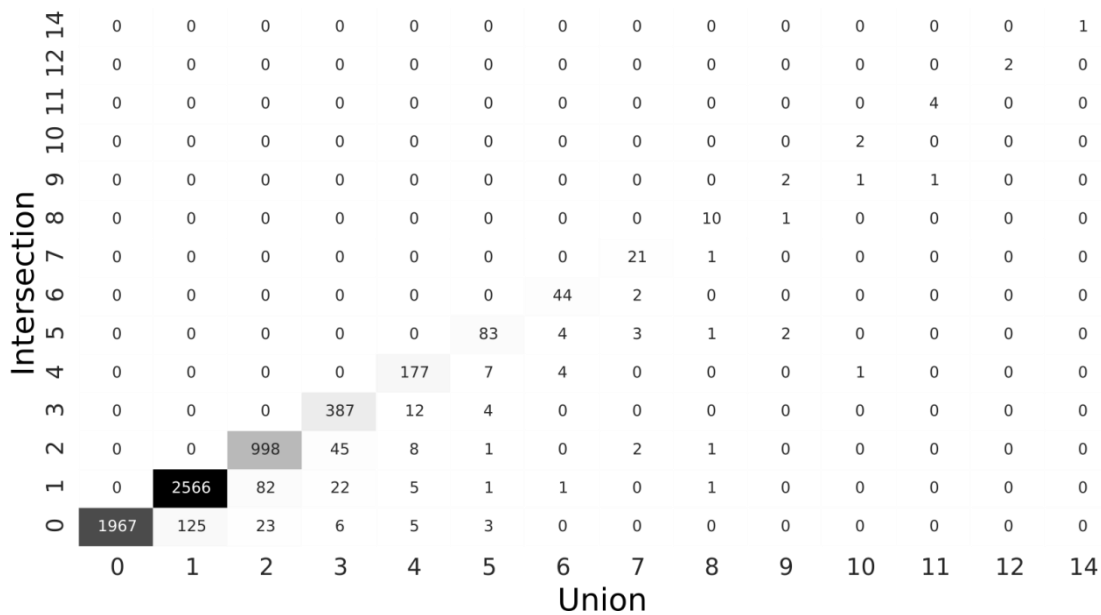
217 We overlay the differentially expressed genes on KEGG pathways using KAAS pipeline [2]. Table  
 218 ST.N.1 shows the pathways which contained differentially expressed genes, together with the genes  
 219 we identify.

220 **Table ST.N.1: KEGG pathways with differentially expressed genes.**

Pathway ID	Pathway	P1 Upregulated	P2 Upregulated
M00360	Aminoacyl-tRNA biosynthesis, prokaryotes	AgabiA15p1   1761, AgabiA15p2   1770 AgabiA15p1   2808, AgabiA15p2   2763	AgabiA15p1   660, AgabiA15p2   686
M00359	Aminoacyl-tRNA biosynthesis, eukaryotes	AgabiA15p1   1761, AgabiA15p2   1770 AgabiA15p1   2808, AgabiA15p2   2763	AgabiA15p1   660, AgabiA15p2   686
M00074	N-glycan biosynthesis, high-mannose type	AgabiA15p1   10048, AgabiA15p2   10102	AgabiA15p1   10047, AgabiA15p2   10101
M00073	N-glycan precursor trimming	AgabiA15p1   10048, AgabiA15p2   10102	AgabiA15p1   10047, AgabiA15p2   10101
M00009	Citrate cycle (TCA cycle, Krebs cycle)	AgabiA15p1   2884, AgabiA15p2   2813	
M00121	Heme biosynthesis, glutamate => protoheme/siroheme	AgabiA15p1   4282, AgabiA15p2   4299	
M00173	Reductive citrate cycle (Arnon-Buchanan cycle)	AgabiA15p1   2884, AgabiA15p2   2813	
M00172	C4-dicarboxylic acid cycle, NADP - malic enzyme type		AgabiA15p1   9348, AgabiA15p2   9524
M00395	Decapping complex		AgabiA15p1   10082, AgabiA15p2   10134
M00179	Ribosome, archaea		AgabiA15p1   9326, AgabiA15p2   9502
M00035	Methionine degradation	AgabiA15p1   8424, AgabiA15p2   8562	
M00010	Citrate cycle, first carbon oxidation, oxaloacetate => 2-oxoglutarate	AgabiA15p1   2884, AgabiA15p2   2813	
M00293	DNA polymerase zeta complex	AgabiA15p1   615, AgabiA15p2   7069	
M00079	Keratan sulfate degradation		AgabiA15p1   9068, AgabiA15p2   9247
M00740	Methylaspartate cycle	AgabiA15p1   2884, AgabiA15p2   2813	
M00042	Catecholamine biosynthesis, tyrosine => dopamine => noradrenaline => adrenaline	AgabiA15p1   7887, AgabiA15p2   8061	
M00128	Ubiquinone biosynthesis, eukaryotes, 4-hydroxybenzoate => ubiquinone		AgabiA15p1   2051, AgabiA15p2   2031
M00338	Cysteine biosynthesis, homocysteine + serine => cysteine	AgabiA15p1   8424, AgabiA15p2   8562	
M00169	CAM (Crassulacean acid metabolism), light		AgabiA15p1   9348, AgabiA15p2   9524
M00178	Ribosome, bacteria		AgabiA15p1   9326, AgabiA15p2   9502
M00295	BRCA1-associated genome surveillance complex (BASC)	AgabiA15p1   1458, AgabiA15p2   1537	
M00012	Glyoxylate cycle	AgabiA15p1   2884, AgabiA15p2   2813	

222 **Supplementary Note O: Differential protein domain annotations**

223 Figure SF.O.1 shows the number of karyollele pairs in which karyollele pairs exhibit different protein  
 224 domain annotations. While most (4287) karyollele pairs have the same number of annotations (see  
 225 the diagonal), a few (215) have different protein domain annotations. This is a result of sequence  
 226 differences.



227

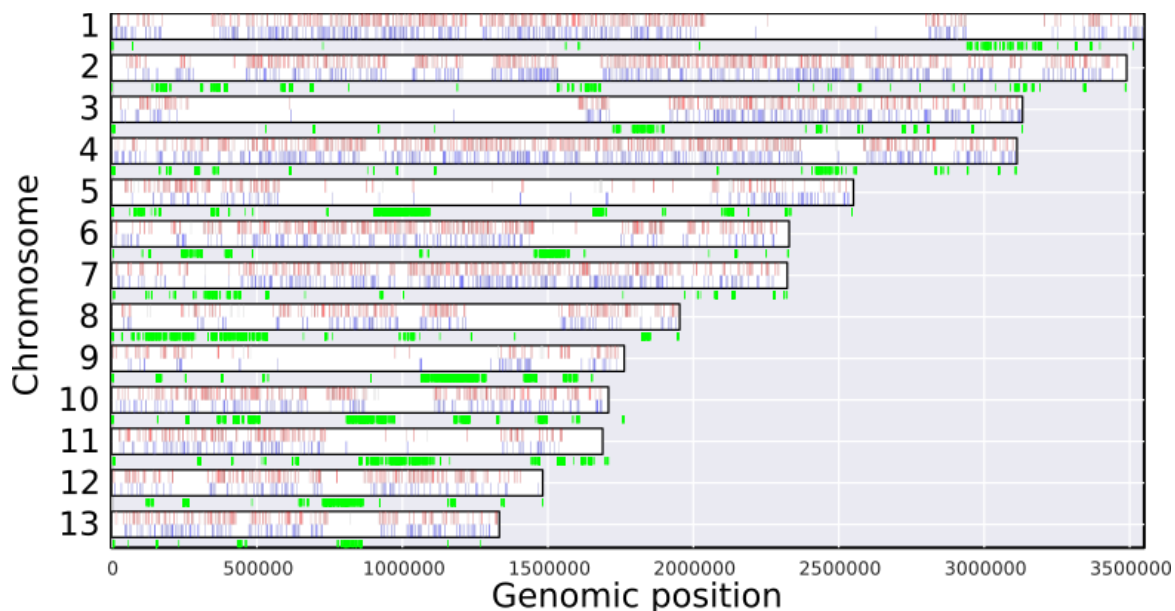
228 **Figure SF.O.1: Implications of sequence deviations between karyollele pairs on domain predictions. The number of**  
 229 **unique annotations are given on the x-axis, and the number of annotations in common between the two karyolleles is**  
 230 **given on the y-axis. If the numbers are not equal, that means that both karyolleles are not annotated with the same**  
 231 **domains. In the corresponding cells are given the number of genes with this combination of annotations. Most genes do**  
 232 **not exhibit alternative functionality (see diagonal), but quite a number do (see below the diagonal).**

233 **Supplementary Note P: PCR duplicates**

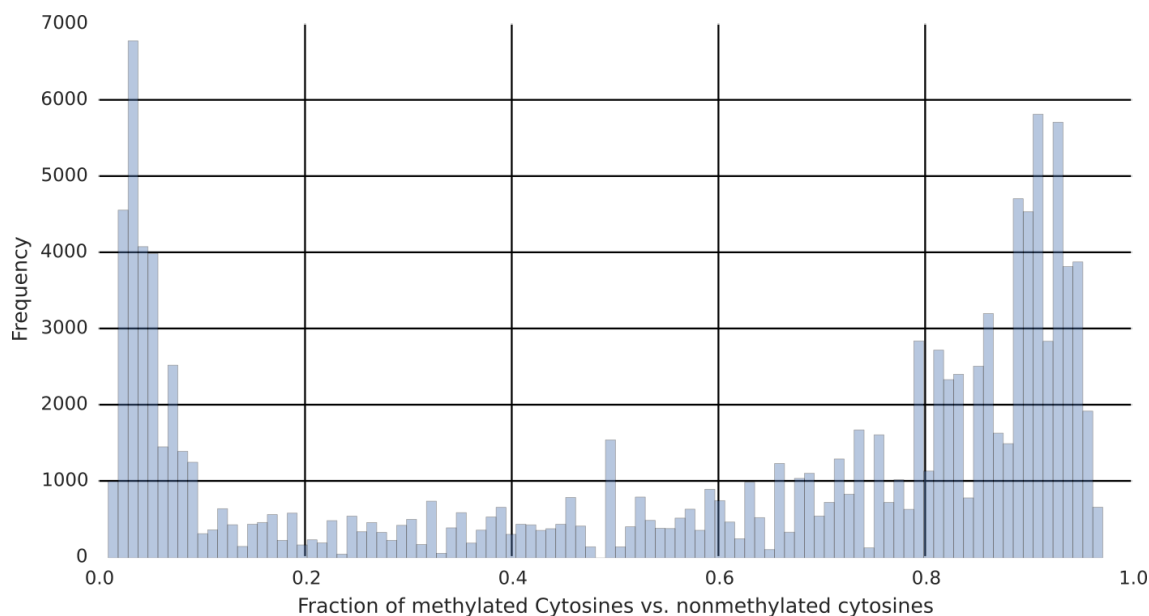
234 PCR duplicates in mushroom tissues dataset and the vegetative mycelium dataset. We find a large  
235 amount of PCR duplication in the compost data. See SupplementaryTable.xlsx, where we provide the  
236 original read counts for each sample, the reads which remain after PCR duplicate removal, and the  
237 percent removed and remaining. We find that the vegetative mycelium dataset contains upwards of  
238 50% PCR duplicates.

239 **Supplementary Note Q: Methylation**

240 Figure SF.Q.1 shows the regions on the genome which are differentially methylated in green. These  
241 mostly overlap with regions that are represented by repetitive elements (Sonnenberg et al. 2016),  
242 where we cannot distinguish genes based in sequence. In Figure SF.Q.2, we show the fraction of  
243 methylated and unmethylated cytosines for a given base. This figure is indicative of an organism  
244 with mixed methylation statuses, which is to be expected in our case.



245  
246 **Figure SF.Q.1: Differentially methylated bases in the A15 genome. As in figure 4 of the main text, the red and blue marks**  
247 **indicate genes with upregulation in the P1 and P2 homokaryons, respectively. The green marks indicate bases which are**  
248 **methylated at that point.**



249  
250 **Figure SF.Q.2: Frequency distribution of methylated vs. non methylated cytosines.**

251

252 **Supplementary Note R: Named genes in *Agaricus bisporus* v. 2**

253 We mapped all transcripts from agabi2 to transcripts P1 with a bidirectional best nucleotide blast  
 254 hit. In one case there was an ambiguous mapping, and we selected the mapping with the highest  
 255 percent sequence identity (the e-values were identical). Table ST.R.1 provides these named genes,  
 256 together with their mapping values.

257 **Table ST.R.1: Named genes in version 2, and their corresponding karyollele pairs in A15.**

P1	P2	agabi2	name	value	pident
AgabiA15p1 9363	AgabiA15p2 9538	152135	AOX	0	98.69
AgabiA15p1 8297	AgabiA15p2 8431	193168	ATP1	0	100
AgabiA15p1 3836	AgabiA15p2 3811	192355	ATP16	0	99.39
AgabiA15p1 8927	AgabiA15p2 9066	139908	ATP17	3.00E-174	98.83
AgabiA15p1 9641	AgabiA15p2 9823	194020	ATP20	0	100
AgabiA15p1 2115	AgabiA15p2 2093	194800	ATP3	0	100
AgabiA15p1 3238	AgabiA15p2 3147	138704	ATP4	0	99.29
AgabiA15p1 6514	AgabiA15p2 6684	135403	ATP7	3.00E-166	98.48
AgabiA15p1 5614	AgabiA15p2 5757	115586	CAT1	0	100
AgabiA15p1 5615	AgabiA15p2 5758	200291	CAT3	0	100
AgabiA15p1 5438	AgabiA15p2 5587	190684	CDC5	0	98.71
AgabiA15p1 3434	AgabiA15p2 3379	121800	CIPB	0	97.33
AgabiA15p1 1432	AgabiA15p2 1515	195535	COX4	0	100
AgabiA15p1 6236	AgabiA15p2 6400	177982	CYP63	0	98.82
AgabiA15p1 7984	AgabiA15p2 8153	135048	CytC2	3.00E-173	100
AgabiA15p1 6030	AgabiA15p2 6190	188638	HMG1	0	99.21
AgabiA15p1 9296	AgabiA15p2 9473	224131	Hpt	0	100
AgabiA15p1 3435	AgabiA15p2 3380	121801	INH1	3.00E-128	98.45
AgabiA15p1 4008	AgabiA15p2 3983	221245	MnP	0	99.06
AgabiA15p1 2172	AgabiA15p2 2148	226574	NDE1	0	100
AgabiA15p1 2932	AgabiA15p2 2853	227697	NDE2	0	100
AgabiA15p1 8485	AgabiA15p2 8625	136834	NUXM	0	100
AgabiA15p1 4154	AgabiA15p2 4172	192611	NUZM	0	98.67
AgabiA15p1 6172	AgabiA15p2 6334	195692	NdufA1	3.00E-123	97.29
AgabiA15p1 6031	AgabiA15p2 6191	139455	NdufA13	0	100
AgabiA15p1 2905	AgabiA15p2 2828	138930	NdufA2	4.00E-133	100
AgabiA15p1 6526	AgabiA15p2 6695	202899	NdufA4	1.00E-122	99.58
AgabiA15p1 646	AgabiA15p2 672	189651	NdufA5	0	98.97
AgabiA15p1 3259	AgabiA15p2 3172	195108	NdufA6	0	99
AgabiA15p1 9358	AgabiA15p2 9534	193806	NdufA9	0	99.45
AgabiA15p1 674	AgabiA15p2 700	214389	NdufB11	7.00E-170	99.39
AgabiA15p1 10070	AgabiA15p2 10123	208065	NdufB7	0	99.72
AgabiA15p1 6069	AgabiA15p2 6226	139429	NdufB9	2.00E-176	99.7
AgabiA15p1 2042	AgabiA15p2 2023	194758	NdufS1	0	100
AgabiA15p1 1088	AgabiA15p2 1111	190005	NdufS3	0	100
AgabiA15p1 9451	AgabiA15p2 9621	193877	NdufS4	0	98.39



AgabiA15p1 601	AgabiA15p2 629	133027	NdufS6	0	99.03
AgabiA15p1 4161	AgabiA15p2 4179	192620	NdufS7	0	100
AgabiA15p1 6033	AgabiA15p2 6193	188636	NdufS8	0	99.16
AgabiA15p1 690	AgabiA15p2 716	133109	Ndufab1	0	98.6
AgabiA15p1 3782	AgabiA15p2 3756	135814	OSCP/ATP5	0	99.08
AgabiA15p1 4327	AgabiA15p2 4346	192776	PAL1	0	99.4
AgabiA15p1 4243	AgabiA15p2 4260	192690	PAL2	0	99.63
AgabiA15p1 3454	AgabiA15p2 3399	210545	QCR2	0	98.58
AgabiA15p1 2199	AgabiA15p2 2174	138465	QCR8	1.00E-161	100
AgabiA15p1 6694	AgabiA15p2 6862	116951	RIM15	0	99.31
AgabiA15p1 3383	AgabiA15p2 3330	195170	SDH4	0	98.02
AgabiA15p1 6899	AgabiA15p2 7121	149788	SSK1	0	100
AgabiA15p1 869	AgabiA15p2 896	114317	STK/HK	0	100
AgabiA15p1 1449	AgabiA15p2 1531	228355	Tco1	0	100
AgabiA15p1 8256	AgabiA15p2 8388	143539	Tco5	0	100
AgabiA15p1 7003	AgabiA15p2 7226	230069	c2h2	0	99.86
AgabiA15p1 4651	AgabiA15p2 4717	203612	frt2	0	97.08
AgabiA15p1 9024	AgabiA15p2 9205	223670	fst4	0	98.9
AgabiA15p1 4515	AgabiA15p2 4547	192934	geranylgeranyl diphosphate synthase	0	97.73
AgabiA15p1 4280	AgabiA15p2 4297	192725	hom2	0	99.28
AgabiA15p1 5529	AgabiA15p2 5676	190759	hspA	0	99.62
AgabiA15p1 4376	AgabiA15p2 4397	192819	hspC	0	99.3
AgabiA15p1 3389	AgabiA15p2 3335	195173	hspD	0	98.77
AgabiA15p1 10959	AgabiA15p2 10986	120944	lcc10	0	91.17
AgabiA15p1 4698	AgabiA15p2 4766	184993	lcc12	0	98.61
AgabiA15p1 1413	AgabiA15p2 1497	139148	lcc2	0	100
AgabiA15p1 4686	AgabiA15p2 4752	184981	lcc3	0	99.89
AgabiA15p1 10961	AgabiA15p2 10987	194714	lcc9	0	85.85